

Electronic supplementary information

Stimulative formation of truncated octahedral LiMn_2O_4 by Cr and Al co-doping for durable cycling Li-ion batteries

Qimei Liang,^{a,b} Zilin Wang,^{a,b} Wei Bai,^{a,b} Junming Guo,^{* a,b} Mingwu Xiang,^{* a,b} Xiaofang Liu,^{a,b} Hongli Bai^{a,b}

^a National and Local Joint Engineering Research Center for Green Preparation Technology of Biobased Materials, Yunnan Minzu University, Kunming, 650500, China

^b Key Laboratory of Green-chemistry Materials in University of Yunnan Province, Yunnan Minzu University, Kunming, 650500, China

The calculation of Li⁺ diffusion coefficient(D_{Li^+}):

The corresponding formula is as follows:¹

$$Z'=R_s+R_{ct}+\delta_w\omega^{-0.5} \quad (1)$$

Further, the D_{Li^+} can be calculated by the following formula:

$$D_{Li^+}=R^2T^2/2S^2n^4F^4C^2\delta_w^2 \quad (2)$$

where the constant values of R and F are 8.314 J/K·mol and 96484.5 C/mol, respectively; the absolute temperature T is 298.15 K; S is the surface area of electrode which is 6.15(cm²); the electron transfer number n is 1; C is the volume concentration of Li⁺ in the spinel LiMn₂O₄ 0.02378 mol/cm³; δ_w is the slope of the line of $Z'\sim\omega^{-0.5}$ (Figure. S10).

The calculation of the apparent activation energy(E_a):

The following formula is generally used to calculate the activation energy (E_a) depend on the EIS data at different temperatures:²

$$i_0=RT/nFR_{ct} \quad (3)$$

$$i_0=A\exp(-E_a/RT) \quad (4)$$

where i_0 means exchange current, the constant values of R and F are 8.314 J/K·mol and 96484.5 C/mol, respectively; the absolute temperature T is 298.15 K; A is an in-dependent coefficient of temperature; the insets in Figure. S11a and b show the Arrhenius plots of $\log i_0$ as a function of 1/T. Based on Eq. (3) and (4), E_a can be expressed in the equation of $E_a=-Rk\ln 10$ (k is the slope of the fitting line in the insets of Figure. S11a and b), thus the activation energies can be further calculated.

References

- 1 Y. Liu, Z. Yang, J. Li, B. Niu, K. Yang and F. Kang, *J. Mater. Chem. A*, 2018, **6**, 13883-13893.
- 2 S. L. Chou, J. Z. Wang, J. Z. Sun, D. Wexler, M. Forsyth, H. K. Liu, D. R. MacFarlane, S. X. Dou, *Chem. Mater.*, 2008, **20**, 7044-7051.

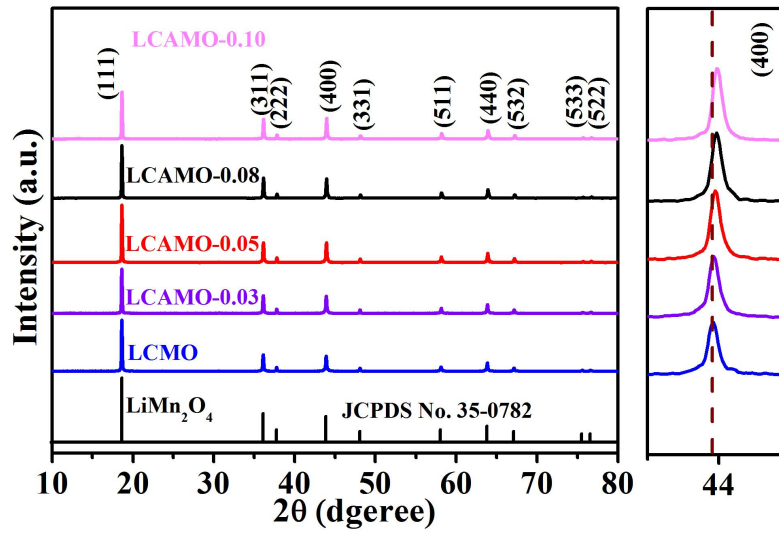


Fig. S1 XRD patterns of all samples along with locally enlarged (400) peaks.

Table. S1 Lattice parameters comparison of all samples

sample	lattice constants (Å)	cell volume(Å ³)	FWHM of (400) peak(°)
LCMO	8.23954	559.38	0.210
LCAMO-0.03	8.23700	558.86	0.206
LCAMO-0.05	8.23353	558.16	0.199
LCAMO-0.08	8.23057	557.56	0.197
LCAMO-0.10	8.22886	557.21	0.187

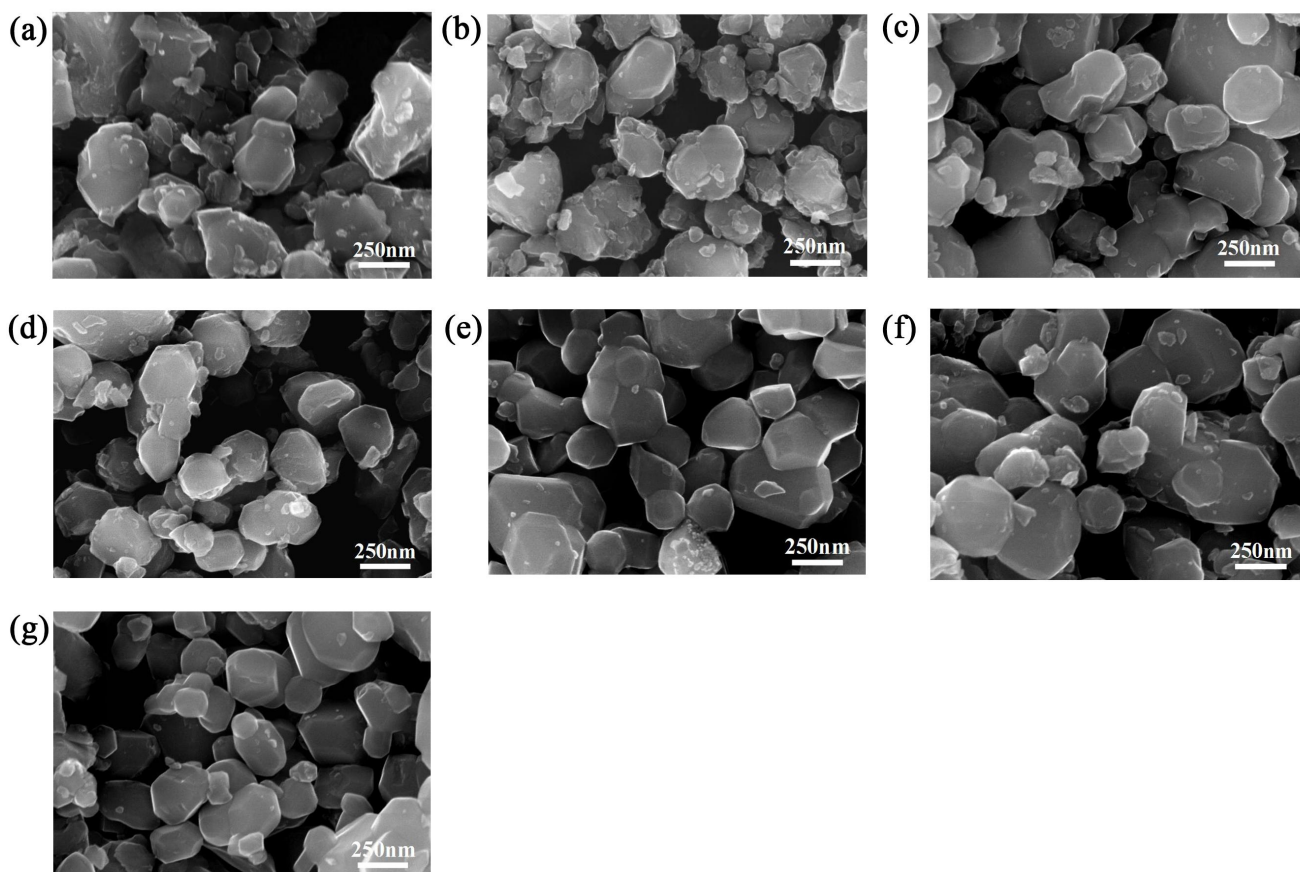


Fig. S2 SEM images of LMO (a), LCMO (b), LAMO (c), LCAMO-0.03 (d), LCAMO-0.05 (e), LCAMO-0.08 (f) and LCAMO-0.10 (g).

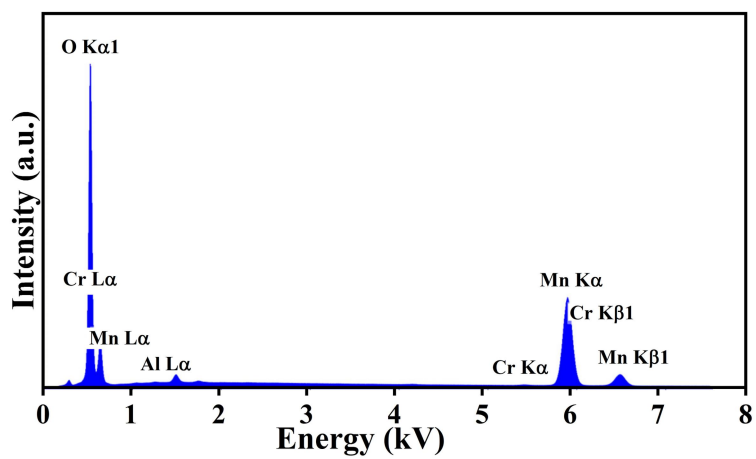


Fig. S3 EDS spectrum of the LCAMO-0.05.

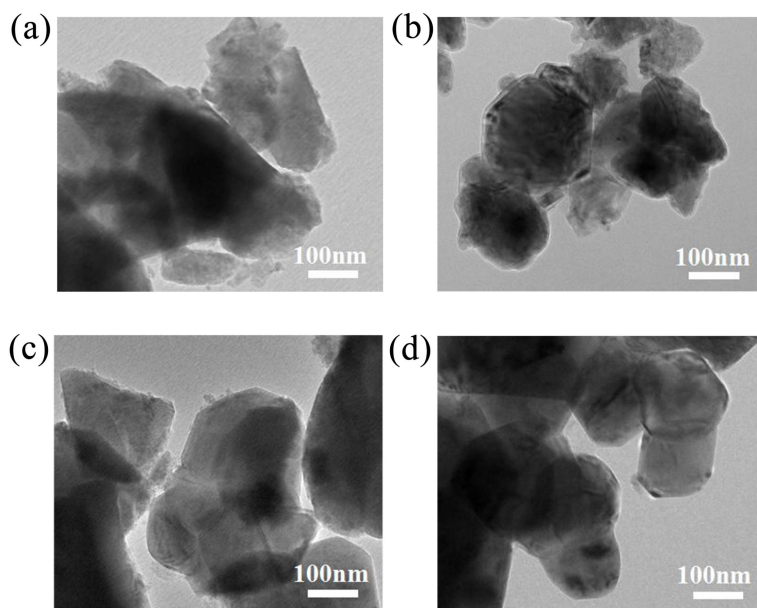


Fig. S4 TEM images of LMO (a), LCMO (b), LAMO (c) and LCAMO-0.05.

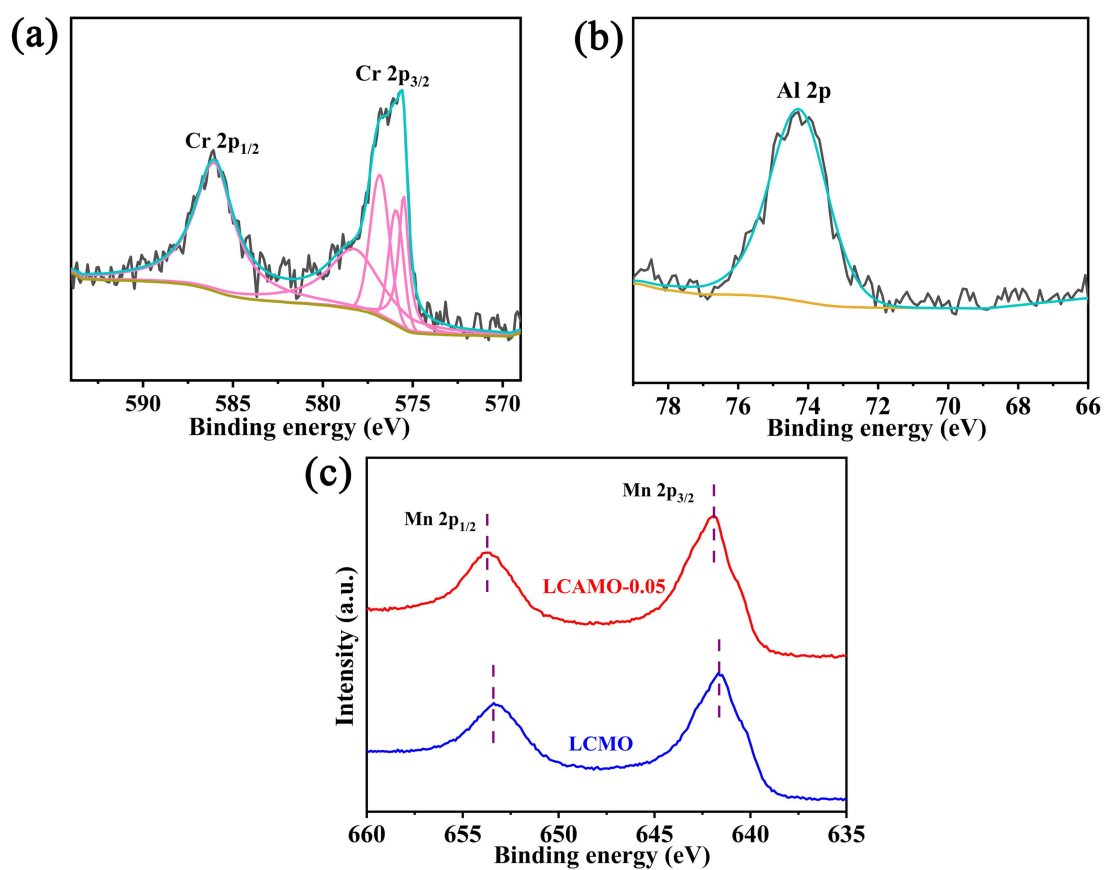


Fig. S5 The high resolution XPS spectra of (a) Cr2p and (b) Al2p of LCAMO-0.05, (c) Mn2p spectra of LCMO and LCAMO-0.05.

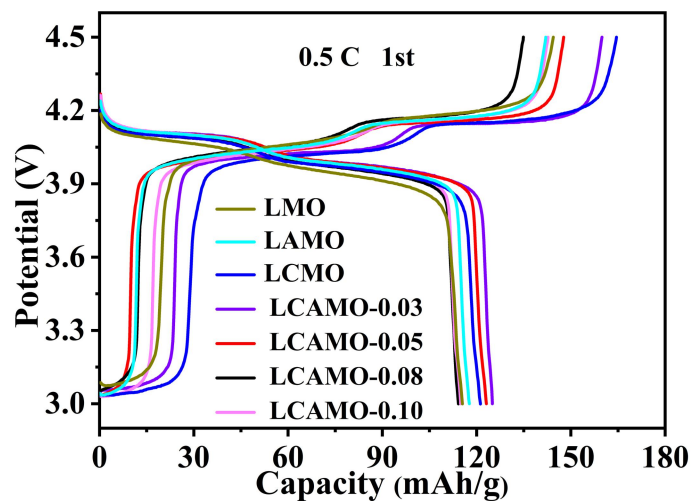


Fig. S6 Initial charge/discharge profiles of all samples at 0.5 C.

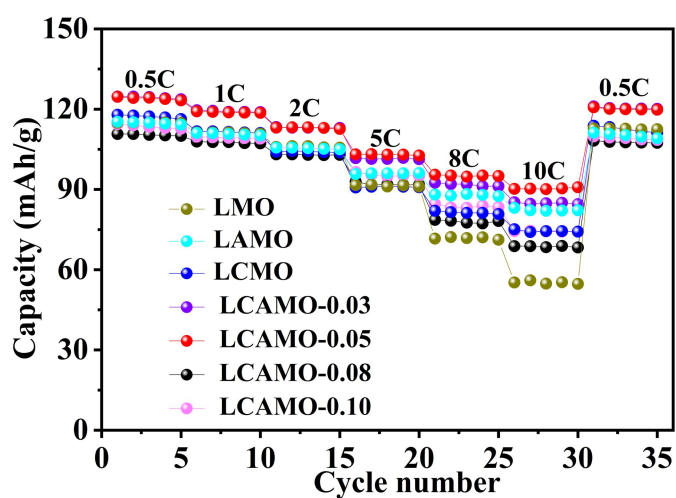


Fig. S7 Rate performances of all samples ranging from 0.5 to 10 C.

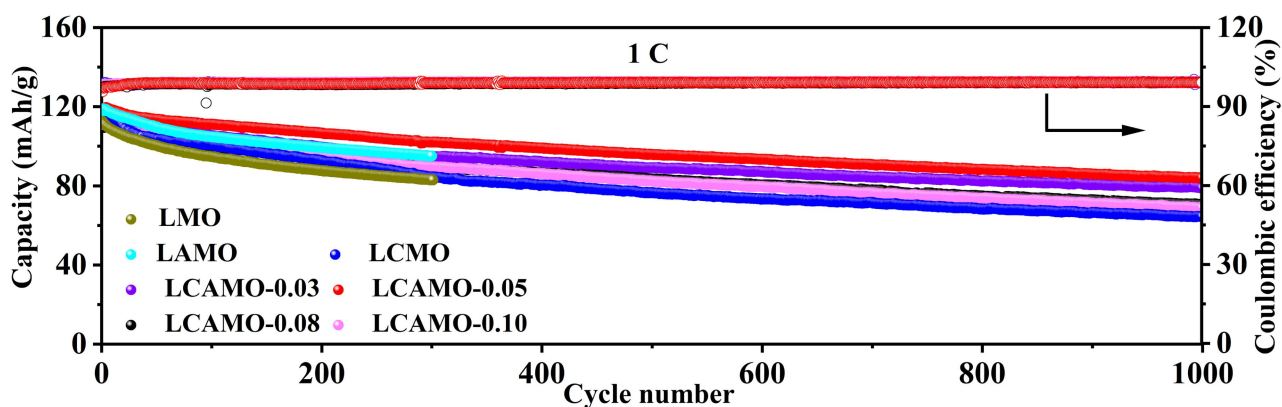


Fig. S8 Cycle performances of all samples at 1 C.

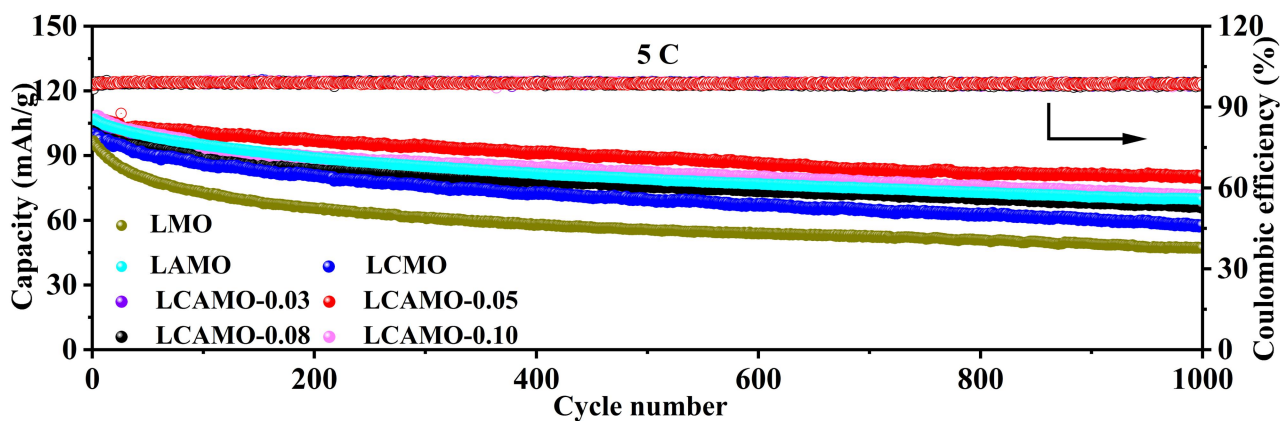


Fig. S9 Cycle performances of all samples at 5 C.

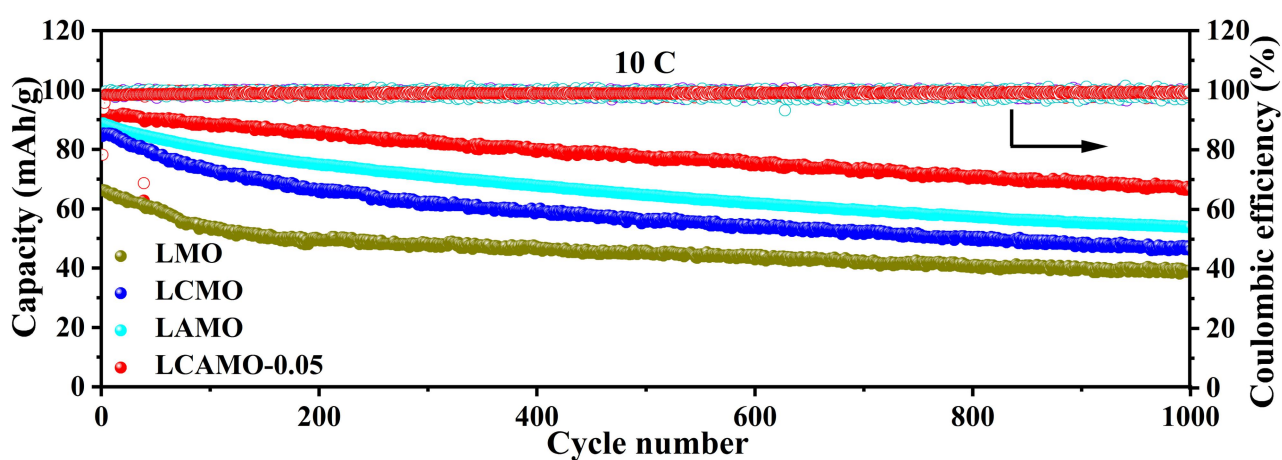


Fig. S10 Cycle performances of LMO, LCMO, LAMO and LCAMO-0.05 at 10 C.

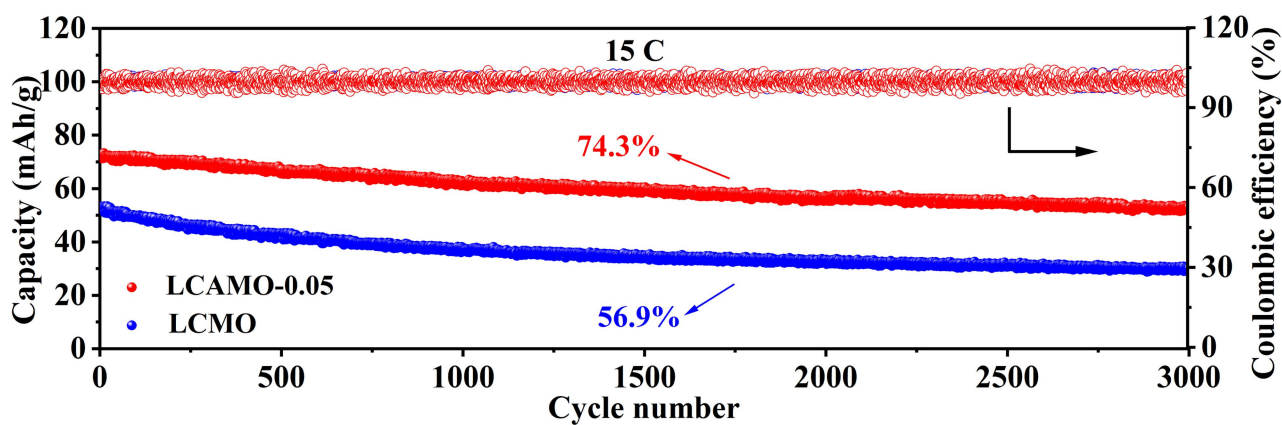


Fig. S11 Cycling performances of LCMO and LCAMO-0.05 at high rate of 15 C.

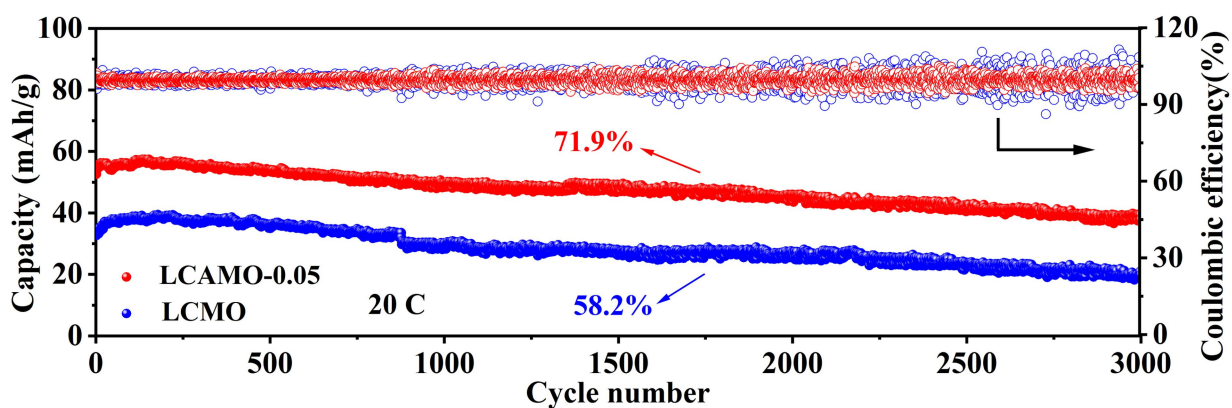


Fig. S12 Cycling performances of LCMO and LCAMO-0.05 at high rate of 20 C.

Table. S2 The charge transfer resistance(R_{ct}), electrolyte resistance(R_s) and ΔR_{ct} [$R_{ct}(\text{before cycle}) - R_{ct}(\text{after cycles})$] values of LCMO and LCAMO-0.05 based on the EIS data before and after 1000 cycles at 5 C

sample	R_s/Ω	R_{ct}/Ω	$\Delta R_{ct}/\Omega$
LCMO	before cycle	1.82	170.6
	after cycles	3.78	340.0
LCAMO-0.05	before cycle	1.50	151.3
	after cycles	3.73	222.0

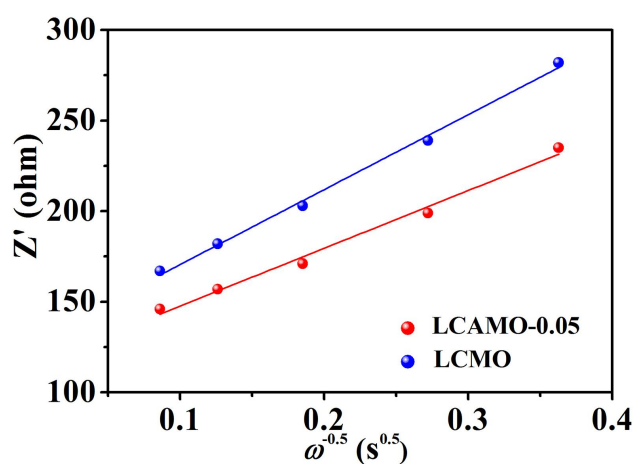


Fig. S13 Fitting curves of the real parts of complex impedance Z' and the $\omega^{-0.5}$

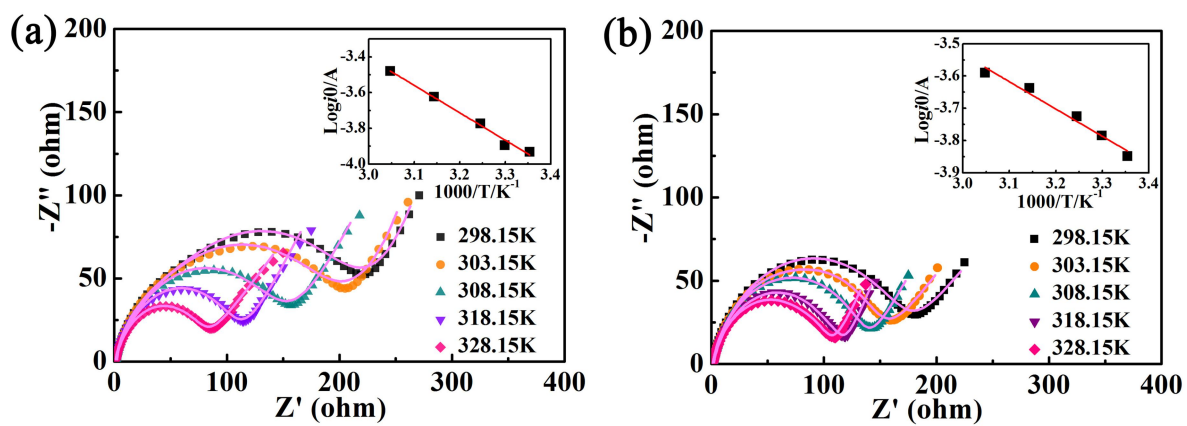


Fig. S14 EIS spectra at different temperatures(25-55 °C) of LCMO (a) and LCAMO-0.05 (b), the insets are the corresponding Arrhenius plots of $\log i_0$ vs. $1000/T$.